International Journal of Smart Grid and Clean Energy

Study on lightning transient behavior of photovoltaic installations

Yaowu Wang[a,*], Ximei Yao[b] , Shiqi Tao[a,] Xiaoqing Zhang[a,] Yanhua Lin[a] , Mengmeng Su[a]

[a] School of Electrical Engineering, Beijing Jiaotong University, Beijing 100044, China
[b] China Association for Standardization, Beijing 100048, China

Abstract

Photovoltaic (PV) system is easy getting stroke for its outdoor characteristics and defendless protective measures. To provide the quantify basis for PV lightning protection formulation, a lightning transient modeling method is presented. With the PV lightning transient model, the lightning transient response that includes the currents on the branches and the potentials at the nodes of PV frame structure could be calculated. The simulated results reveal that the positions of the striking node and the structure of frame system have pronounced influence to the transient responses. The flowing currents on the frame branches closing to the striking node are significantly higher than distant ones. Meanwhile, the transient potential distribution on supporting frame work has an initial distortion and then tends to approximate equalization**.**

Keywords: photovoltaic, lightning transient, framework, lightning protection

1. Introduction

With a rapid growth in photovoltaic power generation, lightning hazard to solar system has drawn strong attentions. The solar systems are easy getting stroke for its outdoor characters: high density of collocated in large scale group and metal frames [1, 2]. For most of the PV frame systems of solar power generations are made of aluminum alloy, it would be a good lightning current path and may damage the PV panels and other devices that linked by cables[3] when getting stroke. Some scholars has used some actual measurement or simulation methods to research the probable lightning damage to solar system [4-8], also the finite difference time domain (FDTD) method has been used to analysis the influence on direct current side of solar energy generations [9, 10], some scholars chose using simulation softwares like CDEGS to simulate the solar system lightning electro-magnetic effects[11].

However, the researches of solar system lightning protection hardly involved the simulation of lightning electric-magnetic transient path on photovoltaic frame system with calculations of branch conductors circuit parameters or whole transient circuit model that included frame system and grounding conductors. Obviously, it's hardly to fulfill the need of solar system lightning protection design that based on lightning transient potential and current responses of solar system without analysis and calculation. With the observed results that usually the actual lightning striking object is PV frame system, and insulations between frame and PV panel may breakdown by overvoltage and overheating by overcurrent. This paper proposed a circuit parameters arithmetic of PV frame conductor branches to build complete PV frame system lightning transient equivalent circuit which included lightning current source model, PV frame system and equivalent grounding conductors model. Then the lightning transient response could be calculated for PV frame system optimization design and solar system lightning protection.

* Manuscript received July 28, 2019; revised November 14, 2019.
Corresponding author. *E-mail address*: 16117407@bjtu.edu.cn.
doi: 10.12720/sgce.9.2.390-396

2. Structural Parameters and Simulation Model

The lightning transient parameters can be calculated on the assumption that the PV frame branches structure is consist of regular cylinders at different spatial positions.

2.1. Capacitance parameters of branch conductor

The capacitance parameters can be calculated with coefficient potential of branch conductors, and which could be calculated by mean potential method, and the ground effect could be solved with method of images [12-13].

Axis out of line of conductor j and k the self-potential coefficient could be calculated with formula 1, and the point of calculate double integral for Λ_{jk} and Λ'_{jk}, and they only relevant with the relative spatial position of conductors. There are 2 categories of conductor spatial position between two conductors or conductor and image conductor, which can be tell apart as parallel and non parallel type as Fig 1 a,b. The calculation of Λ_{jk} and Λ'_{jk} is similarity in mathematics, so just discuss the solution of Λ_{jk} in this paper.

Mutual potential coefficient p_{jk} of any two conductors in space j and k shown in Fig. 1 could be calculated [14].

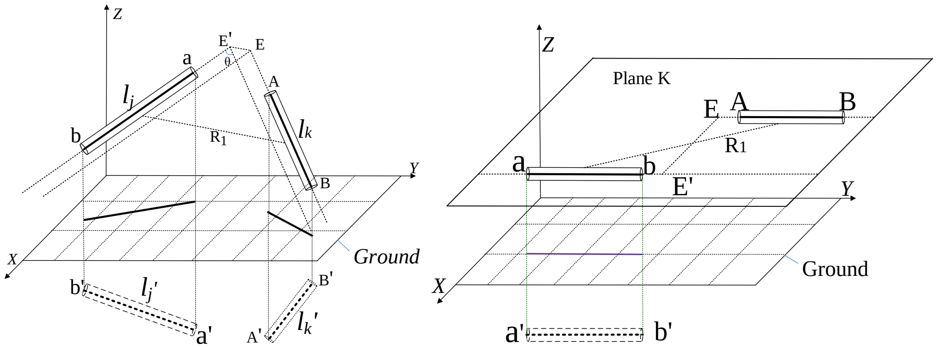

(a) Nonparallel conductor (b) parallel conductor

Fig. 1. Positional relations of space conductors.

$$\begin{aligned} p_{jk} &= \frac{u_{jave} + u_{kave}}{l_j \tau_j} \\ &= \frac{1}{4\pi\varepsilon l_j l_k}\left(\int_{l_j}\int_{l_k}\frac{1}{R_1}dl_j dl_k - \int_{l_j'}\int_{l_k}\frac{1}{R_1'}dl_k dl_j'\right) \\ &= \frac{1}{4\pi\varepsilon l_j l_k}\left(\Lambda_{jk} - \Lambda'_{jk}\right) \end{aligned} \tag{1}$$

where l_j and l_k are the length of conductor j and k respectively, τ_j is the linear charge density of conductor j, k, and ε is the air permittivity.

2.1.1. nonparallel positions

The different surface tilt ubiety can be treated as unmarked case in nonparallel situation, and the rest could deal as special situations of different surface tilt ubieties. As shown in figure 1(a), the two different surface tilt conductors j and k which terminal vertex are a, b and A, B, and the length of j and k are *l* and *m* separately, R_1 is the distance between j and k, and the Λ_{ij} can be calculate as formula 2.

$$\begin{aligned} \Lambda_{jk} &= \int_{l_k}\int_{l_j}\frac{1}{R_1}dl_j dl_k \\ &= (d_2 + l)\ln\frac{d_4 + d_5 + m}{d_4 + d_5 - m} - \\ & d_2 \ln\frac{d_6 + d_7 + m}{d_6 + d_7 - m} + (d_3 + m)\ln\frac{d_4 + d_7 + l}{d_4 + d_7 - l} - \\ & d_3 \ln\frac{d_5 + d_6 + l}{d_5 + d_6 - l} - \frac{\delta d}{\sin\theta} \end{aligned} \tag{2}$$

where

$$\begin{aligned}\delta = &\tan^{-1}\left(\frac{d_1}{d_4\tan\theta}+\frac{(d_2+l)(d_3+m)\sin\theta}{d_1d_4}\right)-\\&\tan^{-1}\left(\frac{d_1}{d_5\tan\theta}+\frac{(d_2+l)d_3\sin\theta}{d_1d_5}\right)+\\&\tan^{-1}\left(\frac{d_1}{d_6\tan\theta}+\frac{d_2d_3\sin\theta}{d_1d_6}\right)-\\&\tan^{-1}\left(\frac{d_1}{d_7\tan\theta}+\frac{d_2(d_3+m)\sin\theta}{d_1d_7}\right)\end{aligned} \tag{3}$$

d1, d_2, d_3, d_4, d_5, d_6, d_7 are the length of line E'E, EA, E'a, Bb, Ba, Aa, Ab in Fig.1a respectively.

When $\theta\neq\pi/2$ and $\delta d/\sin\theta=0$, Λ_{jk} is the integral of conductors in coplane tilt situation;

When $\theta=\pi/2$ and $\delta d/\sin\theta\neq 0$, Λ_{jk} is the integral of conductors in different surface vertical situation;

When $\theta=\pi/2$ and $\delta d/\sin\theta=0$, Λ_{jk} is the integral of conductors in coplane vertical situation.

2.1.2. parallel positions

As shown in Fig. 1b, the parallel conductors j and k which terminal vertex are a, b and A, B, the length of j and k are *l* and *m* separately, d_8 and d_9 are the length of line Eb and AE respectively, then the Λ_{jk} can be calculated as below.

$$\begin{aligned}\Lambda_{jk} &= \int_{l_k}\int_{l_j}\frac{1}{R_1}\mathrm{d}l_j\mathrm{d}l_k\\&= (l+d_9+m)\sinh^{-1}\frac{l+d_9+m}{d_8}-\\&\sqrt{(l+d_9+m)^2+d_8^2}+d_9\sinh^{-1}\frac{d_9}{d_8}-\sqrt{d_8^2+d_9^2}-\\&(m+d_9)\sinh^{-1}\frac{m+d_9}{d_8}+\sqrt{(m+d_9)^2+d_8^2}-\\&(l+d_9)\sinh^{-1}\frac{l+d_9}{d_8}+\sqrt{(l+d_9)^2+d_8^2}\end{aligned} \tag{4}$$

Based on the spatial location, circuit potential parameters of the conductors could be calculated. Setting the PV frame system consist of n positive coupling branch conductor units, and the potential coefficient matrix is $\boldsymbol{P}$.

$$\boldsymbol{P} = \{p_{jk}\}_{\mathrm{n,n}} \tag{5}$$

Inverse the matrix $\boldsymbol{P}$,

$$\boldsymbol{P}^{-1} = \{p'_{jk}\}_{\mathrm{n,n}} \tag{6}$$

With the definition of capacitance, n positive coupling branch conductors' capacitance matrix $\boldsymbol{C}=\{C_{jk}\}_{\mathrm{n,n}}$ could be calculated.

$$\begin{aligned}C_{jj} &= \sum_{j=1}^{n}p'_{jk} \qquad (j=1,2\cdots k\cdots n-1,n)\\C_{jk} &= -p'_{jk} \qquad (j,k=1,2\cdots n, k\neq j)\end{aligned} \tag{7}$$

2.2. Inductance and resistance of branches conductors

Based on the principle of electromagnetic similarity, branches inductance matrix $\boldsymbol{L}$ could gotten from the $\boldsymbol{C}$ matrix [15].

$$\boldsymbol{L} = \mu_0\varepsilon_0\boldsymbol{C}^{-1} \tag{8}$$

On the assumption that *p* is the serial number of any single branch conductor in PV frame system, the resistance shall consider the effects of high frequency components of thunder frequency spectrum[16].

$$R_{\mathrm{p}} = \frac{l_{\mathrm{p}}\sqrt{\mu f_{\mathrm{e}}}}{2r\sqrt{\pi\sigma_{\mathrm{c}}}} \tag{9}$$

where σ_c is the conductivity of the branches conductors, μ is the magnetic conductivity of the conductor, f_e is upper cut-off frequency, l_p is the length of p conductor, r is the frame conductor radius calculate by equivalent area method.

With the parameters of RLC, any branch coupling conductors could expressed as a coupled π equivalent circuit, and j and k conductors which shown in Fig. 2 expressed the basic layout π equivalent circuit of any two coupled branches conductors of PV frame system.

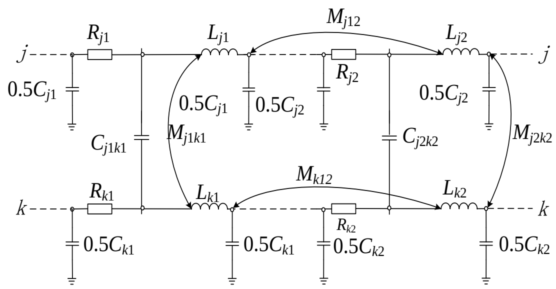

Fig. 2. PV frame equal π style coupled circuits

3. Simulation Example

Based on the lightning protection standard, chose the lightning current waveform parameter as 10/350 us, 100 kA [17], and the PV frame system parameters shown in Fig. 3.

Chose the cliff-corner of PV frame as the lightning strike node for it's the easiest node getting stroke, and simplify the grounding system to vertical earthing conducting system as 7 Ω, with all these presupposition, the complete PV frame transient circuit is built which is shown as Fig.4. Then the transient responses on the frame could be calculated with the software EMTP-RV.

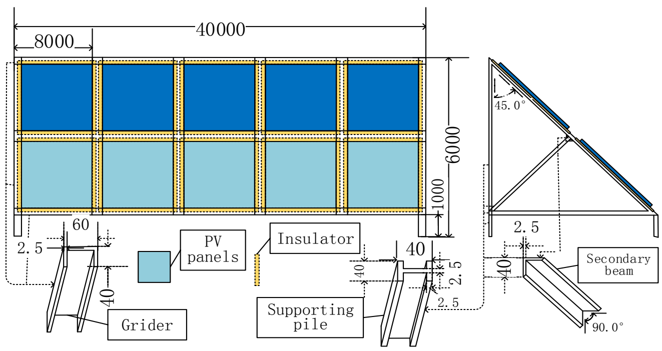

Fig. 3. Example parameter, unit(mm)

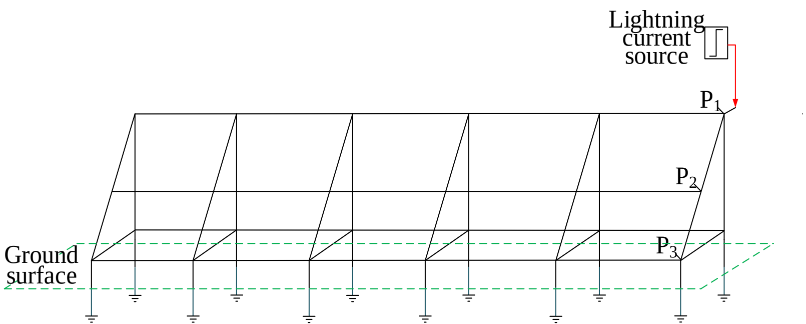

Fig. 4. PV frame simulation diagrammatic

3.1. potential waveform on different position of PV frame system

Chose observation points P1~P3 in Fig. 4, the potential waveform are shown in figure 5.

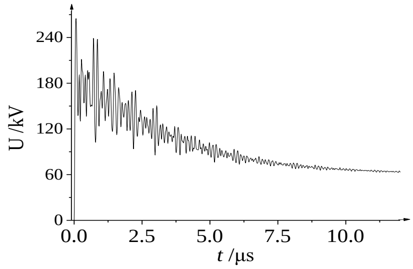

(a) P1 position

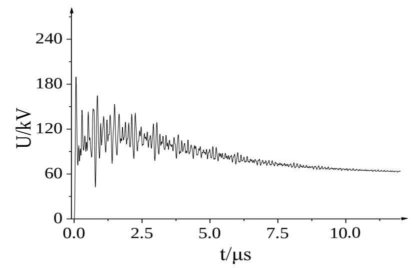

(b) P2 position

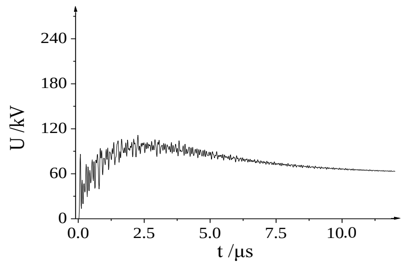

(c) P3 position

Fig. 5. Potential waveforms on PV frame

3.2. Transient response spatial and temporal distribution on PV frame system

The simulation results of lightning electric transient response on typical moment as 0.1 μs, 10 μs and 350 μs shown in Fig.6.

To facilitate analysis the lightning transient on PV frame system, we introduce a coefficient γ as transient shunt ratio, define it as the ratio of amplitude of transient current on a branch of PV frame system to the lightning injection current, which is using to representing the transient current distribution on the PV frame system, and the transient potential value is shown in color. From figure 6, we can see when it's 0.1 μs after the strike, the distribution of transient current is very unbalanced, and on a high distortion degree, the γ is much bigger than further branches from the strike point, and the grounding current is mainly flow through the stake that near the strike point; when it is 10 μs, the distortion distribution of transient current is significantly reduced, and the current extend to further; and when it's 350 μs, the distribution on the PV frame system has been basically balanced, and even the furthest branch from the strike point has played a certain role of shunt.

By the transient potential distribution that distinguished by color, it can be seen that the peak value of whole time show up when 0.1 μs, and the distribution of the potential is unevenly, the value is rapidly declined with the distance to the strike point; when it's 10 μs, the potential value of conductors on each branch of the PV frame is tend to be balanced, but the maximum potential value is far less than the peak; when it's 350 μs, the potential of each branch conductor is basically the same and drops steadily.

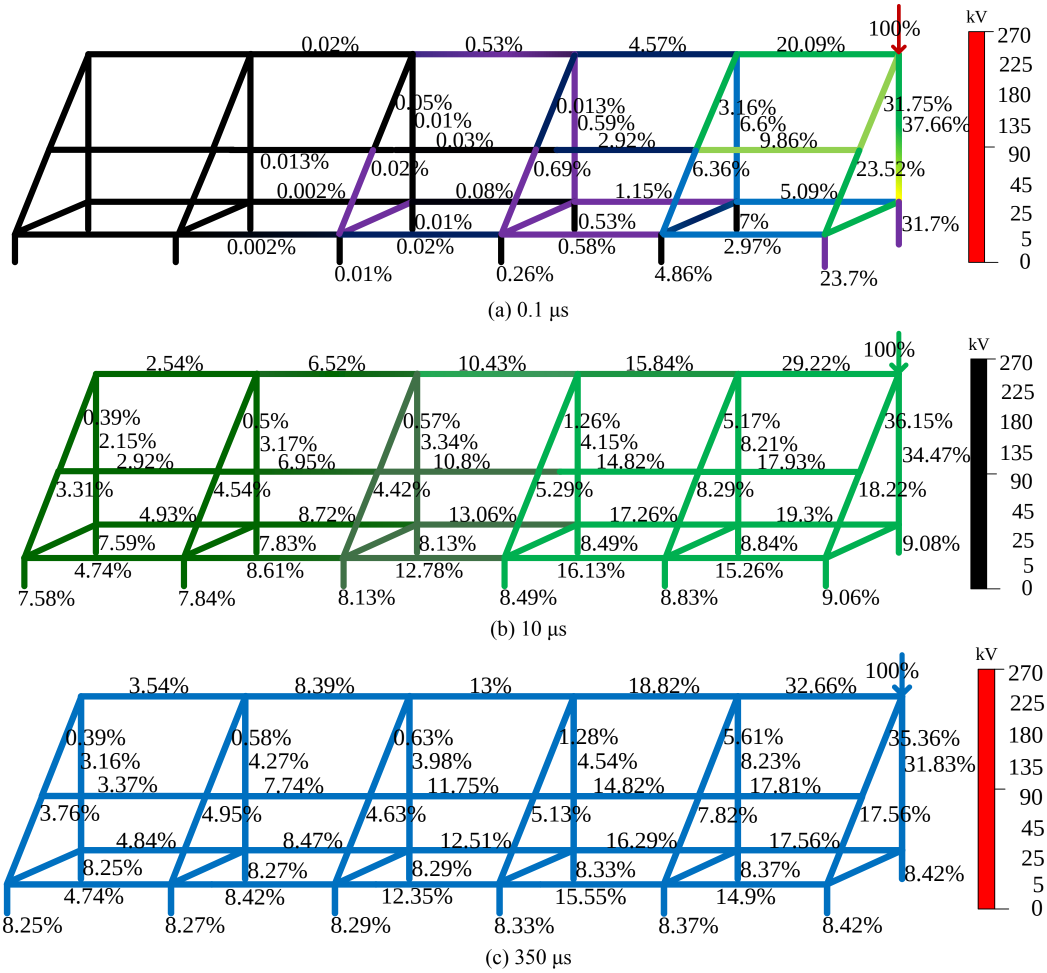

Fig.6. Lightning transient distribution on PV frame structure

4. Conclusion

This paper presented a method to calculate the circuit parameters of complex space branches of PV frame system, and complete the lightning transient PV frame system circuit model, then calculate the transient responses on PV frame system with actual size example . With the distribution of lightning transient responses on PV frame system , conclusions can be draw as:

At initial period, the transient potential soon get highest value and rise to kV level at the lightning strike node. But with the distance increase, transient potential value declined rapidly till to zero. With the transient process continue, the value of transient potential continuous declined on whole PV frame. It's basically balanced when half peak moment, the max-voltage between frame branches are less than 1.4% of mean potential.

On the PV frame system, the peak value of the transient current through the branches are related to the spatial distances to the lightning strike point as low in the distance and high on the contrary. On the process of lightning transient, the difference value of current transient shunt ratio decrease from 37.1% at the initial period to 0.2% when it's half peak value moment, the distribution of transient current is basically balanced.

The method that presented in this paper can be applied in large-scale PV array field for lightning protection.

Conflict of Interest

The authors declare no conflict of interest.

Author Contributions

Wang conducted the research; Yao, Tao and Zhang wrote the paper; Lin and Su analyzed the data. All authors had approved the final version.

Acknowledgements

This work is partly supported by National Natural Science Foundation of China under Grant No. 51777007.

References

[1] Ahmad NI, Ab-Kadir MZA, Izadi M, et al. Lightning protection on photovoltaic systems: A review on current and recommended practices. *Renewable & Sustainable Energy Reviews*, 2017; 82.

[2] Christodoulou CA, Ekonomou L, Gonos IF, et al. Lightning protection of PV systems. *Energy Systems*, 2015; 7(3):1-14.

[3] Bower WI, Wiles JC. Analysis of grounded and ungrounded photovoltaic systems. In: *IEEE Photovoltaic Specialists Conference - 1994, 1994 IEEE First World Conference on. IEEE*, 1994: 809-812.

[4] Belik M. PV panels under lightning conditions. In: *Proc. of the 2014 International Scientific Conference on Electric Power Engineering. IEEE*, 2014; 367-370.

[5] Dechthummarong C, Chenvidhya D, Jivacate C, et al. Experiment and simulation impulse partial discharge behavior in dielectric encapsulations of field-aged PV modules. In: *Photovoltaic Specialists Conference. IEEE*, 2011; 3109-3112.

[6] Jiang T, Grzybowski S. Impact of lightning impulse voltage on polycrystalline silicon photovoltaic modules. In: *International Symposium on Lightning Protection. IEEE*, 2014; 287-290.

[7] Tamura K, Araki K, Kumagai I, et al. Lightning test for concentrator photovoltaic system. In: *Photovoltaic Specialists Conference. IEEE*, 2011; 996-998.

[8] Hernández JC, Vidal PG, Jurado F. Lightning and surge protection in photovoltaic installations. *IEEE Transactions on Power Delivery*, 2008; 23(4):1961-1971.

[9] Yamamoto K, Takami J, Okabe N. Overvoltages on DC side of power conditioning system caused by lightning stroke to structure anchoring photovoltaic panels. *Electrical Engineering in Japan*, 2014; 187(4):29–41.

[10] Stern HJ, Karner HC. Lightning induced EMC phenomena in photovoltaic modules. In*:IEEE International Symposium on Electromagnetic Compatibility, 1993. Symposium Record. IEEE Xplore*, 1993; 442-446.

[11] Sueta HE, Mocelin A, Zilles R, et al. Protection of photovoltaic systems against lightning experimental verifications and techno-economic analysis of protection. In*:International Symposium on Lightning Protection. IEEE*, 2013; 354-359.

[12] Richard Phillips Feynman. *The Feynman Lectures on Physics*. Beijing: Higher Education Press; 2000.

[13] Tao S, Zhang X, Wang Y. Transient behavior analysis of offshore wind turbines during lightning strike to multi-blade. *IEEE Access*, 2018; (99).

[14] Iosseli UY, Kothanof AS, and Stlyrski MG, Calculation of capacitances, *Electric Power Press*, Moscow, Russia, 1991.

[15] Ametani A, Kasai Y, Sawada J, Mochizuki A, Yamada T. Frequency-dependent impedance of vertical conductors and a multiconductor tower model, In: *IEEE Proceedings-Generation, Transmission and Distribution 1994*; 141: 339-345.

[16] Shiqi T, Xiaoqing Z. Analysis of transient responses on wind turbines during direct lightning strike. *Acta Energiae Solaris Sinica*, 2017; 38 (10):2675-2682.

[17] IEC62305—2（Protection against lightning Part 2：Risk Management）